Removal of oxygen from (bio-)methane via catalytic oxidation of CH$_4$—Reaction kinetics for very low O$_2$:CH$_4$ ratios

Felix Ortloff [a,*], Jan Bohnau [a], Frank Graf [a], Thomas Kolb [a,b]

[a] DVGW Research Center at Engler-Bunte-Institute (DVGW-EBI), Karlsruhe Institute of Technology (KIT), Engler-Bunte-Ring 1, 76131 Karlsruhe, Germany
[b] Engler-Bunte-Institute, Fuel Technology Division (EBI ceb), Karlsruhe Institute of Technology (KIT), Engler-Bunte-Ring 1, 76131 Karlsruhe, Germany

ARTICLE INFO

ABSTRACT

For evaluation of design specifications for catalytic oxygen removal units, examinations on reaction kinetics of catalytic oxidation of methane at very low O$_2$:CH$_4$ ratios have been performed in the temperature range between $200 < T < 350\,°C$ and pressures below 10 bar, applying a commercial noble metal (Pt) Al$_2$O$_3$-based catalyst. On the basis of the experimental results, a mass based rate equation is proposed, taking into account the influence of both, reactants and products of the reaction on the conversion rate of oxygen. This equation is valid for oxygen inlet pressures of as low as 1 mbar and has further been tested in a balance of methane of up to $p_{CH_4} = 10$ bar (abs.).

For comparison of conversion rates of oxygen with various other reductives, such as ethane, propane and butane, equivalent experiments were performed and kinetic parameters of corresponding power law approaches are given. Finally, the catalytic activity of further noble metals and some transition metal catalysts was tested and compared to the platinum reference catalyst.
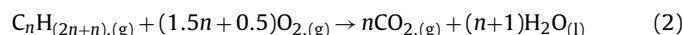
© 2015 Elsevier B.V. All rights reserved.

1. Introduction

In Europe, in particular in Germany, strong efforts have been undertaken to increase the share of renewables in power supply. In Germany approximately 160 biogas injection plants with an overall injection capacity of about 800 million m^3/a are in operation [1]. On the way towards a further increase of the overall biogas capacity in Europe and due to seasonal fluctuation of natural gas sales, an increasing amount of biogas will have to be fed and stored in the gas transportation network (MOP > 16 bar). In order to prevent damage to the gas infrastructure (e.g., by corrosion [2]), the maximum oxygen concentration is limited to 10 ppmv for transportation pipelines connected to underground storages and/or cross border transmission [3–5].

In recent monitoring programs, residual oxygen contents in biogas in a range between 0.1 up to 1.8 vol% with an average of around 0.5 vol% have been reported [6]. Critical points of oxygen intake have been identified and recommendations on the optimization of the biogas upgrading chain for preventing oxygen intake have been given. Since a small remaining amount of oxygen in biogas is inevitable, options for removal are necessary [7].

By now, traces of oxygen are removed by chemisorption based processes (e.g., copper or chromium based adsorbents are applied). Higher amounts of oxygen in fuel gas streams are treated by catalytic oxidation of either hydrogen (Eq. (1)) or (e.g., in natural gas applications) hydrocarbons (C$_n$H$_{n+2}$ with $n > 2$, Eq. (2), Table 1) [8].

$$2H_{2,(g)} + O_{2,(g)} \rightarrow 2H_2O_{(l)} \tag{1}$$

$$C_nH_{(2n+n),(g)} + (1.5n + 0.5)O_{2,(g)} \rightarrow nCO_{2,(g)} + (n+1)H_2O_{(l)} \tag{2}$$

One promising alternative for the removal of oxygen from biogas is the catalytic oxidation of methane (Eq. (3)), which is available in-situ in biogas and therefore does not have to be supplied, stored and added to the gas stream separately. Besides, in case of biogas, the utilization of methane appears to be the most sustainable and, due to higher temperatures applied to the catalyst, the more robust option in view of trace compounds of biogas, e.g., sulfur containing contaminants.

$$CH_{4,(g)} + 2O_{2,(g)} \rightarrow CO_{2,(g)} + 2H_2O_{(l)} \tag{3}$$
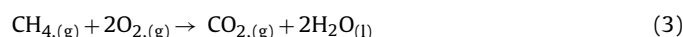
Certainly, the catalytic oxidation of methane is widespread in industry and has been under intensive research for decades. By now, it is basically used within two fields of application:

Nomenclature

Θ	Surface coverage (–)
a	Mass specific surface area (m²/g)
A	Order of reaction of oxygen (–)
B	Order of reaction of various fuel gases (–)
Bo	Bodenstein number (–)
C	Constant (–)
d	Diameter (mm)
E_A	Activation energy (kJ/mol)
h	Height of the catalytic bed (mm)
$\Delta_R H^{\Theta}$	Standard enthalpy of reaction (kJ/mol)
$\Delta_{ads} H^{\Theta}$	Standard enthalpy of adsorption (kJ/mol)
k_0	Reaction rate constant (mass specific) (mol/(s g bar^B))
K_0	Equilibrium constant (bar^{-C})
m_{ac}	Mass of active compound (g)
n_i	Moles of i (mol)
p_i	(Partial) pressure (of i) (bar)
$r_{m,i}$	Mass specific reaction rate (mol/(s g bar^B))
R	Universal gas constant 8.314 kJ/ (kmol K))
t	Time (s)
T_R	Reaction temperature (K)
$\dot{V}$	Volumetric flow rate (m³/s)
Wz	Weisz modulus (–)
X_i	Conversion of i (–)
y_i	Mole fraction of i in the gas phase (–)

Table 1
Heats of combustion for oxidation of various fuel gases.

$\Delta_R H^{\Theta}$ kJ/mol	H_2	CH_4	C_2H_6	C_3H_8	C_4H_{10}
	−571.6	−890.5	−1560	−2220	−2877

- Catalytic exhaust gas treatment systems, operated in excess of oxygen, e.g., in the transportation sector [9]
- Catalytic burners, operated close to the stoichiometric necessary amount of oxygen [10–12].

The actual challenge of this work is the uncommon gas composition in terms of its very low content of oxygen, typically ranging below 1 vol%, in large excess of fuel gas.

For catalytic combustion, noble metals show the highest activity, whereby in industry mainly palladium and platinum are used [13]. Due to economic reasons, some comparably less active transition metals [14], their corresponding oxides [15,16], mixtures of catalyst materials [17] or perovskites [18] are also applied. Besides the activity of the actual catalytic materials, the influences of e.g., catalyst support, promoters, physical properties, such as surface area or pore structure, or even formulation process are discussed in literature [19].

For modelling the reaction rate of the catalytic combustion of methane, different approaches are discussed in literature. The Langmuir–Hinshelwood mechanism [20] presumes that both reactants, methane and oxygen, are adsorbed on the surface of the catalyst before the reaction can take place. The Eley–Rideal mechanism postulates, that dissociated oxygen is present in large surplus on the catalytic surface of noble metal catalysts at any time [21]. Hence, oxygen partial pressure often has almost no influence on the reaction rate. However, methane reacts from the gas phase or from a weakly adsorbed state, which leads to a strong dependence on the partial pressure of the fuel gas.

After adsorption, pyrolytic and oxidative methane decomposition are discussed as competitive reactions on the surface of the catalyst [22]. In case of palladium, a Mars–van-Krevelen mechanism is proposed, where palladiums bulk oxygen is involved [23]. The formation of methyl species is commonly assumed as the overall rate determining reaction step [24].

Besides, the products of the reaction, water vapor [13,25] and carbon dioxide [13] , show inhibiting effects on the reaction rate, as their adsorption competes with the adsorption of the reactants. Water vapor shows a higher affinity to the active sites than CO_2, resulting in a stronger decrease in methane conversion rate [13].

The described findings are approved for the two aforementioned common applications of the catalytic combustion of methane, namely exhaust gas treatment and catalytic burners. In the context of oxygen removal from biogas, applicability is uncertain and therefore was examined in this work. The focus of this work lies on the utilization of methane as a reducing agent and its conversion on platinum, whereby the results are compared with other reductives and other noble or transition metal based catalysts.

2. Experimental

2.1. Materials

In this work, a platinum catalyst was used as a benchmark for catalytic activity. The catalyst is based on a commercially available product from Heraeus precious metals GmbH, Hanau, Germany. As active compound, 0.5 wt% of Pt are dispersed on a spherical catalyst support of Al_2O_3 with an outer diameter of 1–1.2 mm and a BET surface area a_{BET} of 173 m²/g (measured with a micromeritics ASAP 2020 physisorption analyzer).

Furthermore, catalytic activity of other noble and transition metals was studied. For transition metal catalysts, a reduction method with hydrogen (12 h, 400 °C) was applied in advance of the actual experiments on oxygen removal. Details on the applied catalysts are given in Table 2. In order to reduce heat production density in the reactor during the experiments, all examined catalysts were diluted with Al_2O_3-spheres, which basically are the uncoated catalyst support.

Table 3 shows the gases applied for the kinetic measurements and for comparison of catalysts. For water vapor dosing, de-ionized water was used.

Table 2
Applied catalysts and configuration during measurements.

Catalyst	wt% Active compound	Support	a_{BET} (m²/g)	Supplier
Platinum	0.5	Al_2O_3	173	Heraeus
Palladium	0.5	Al_2O_3	182	Heraeus
Rhodium	0.5	Al_2O_3	172	Aldrich
Copper	0.5	Al_2O_3	178	Heraeus
Silver	0.5	Al_2O_3	152	Heraeus
Dilution material	–	Al_2O_3	179	Heraeus

Table 3
Applied gases with information on respective purities and suppliers.

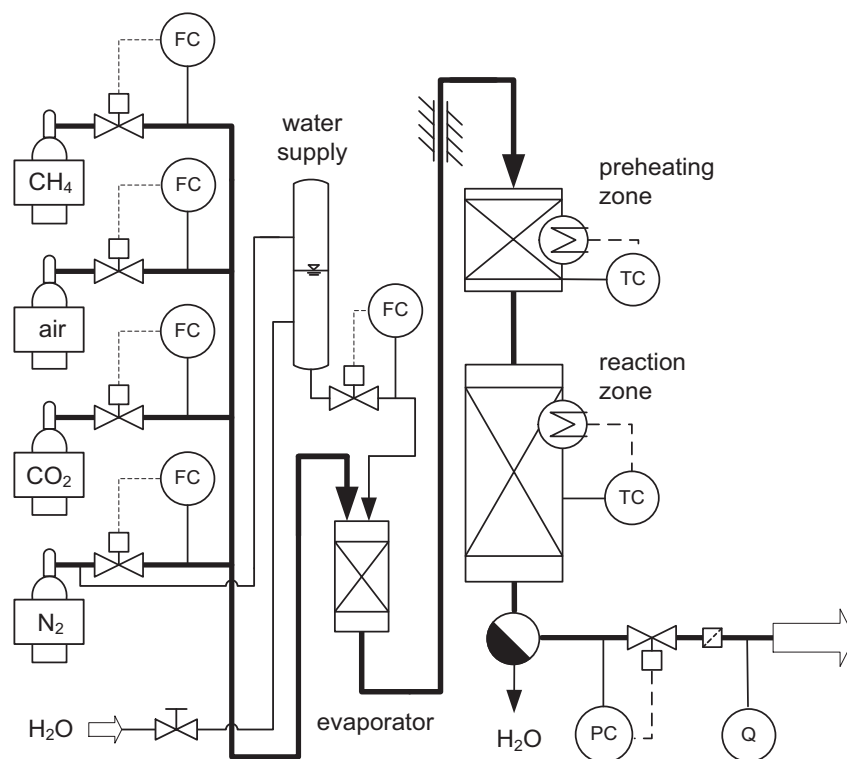| Compound	Purity
Methane	3.5 (99.95 vol %)
Synthetic air (20.5 vol% O_2 in N_2)	99.9997 vol%
Nitrogen	5.0 (99.999 vol %)
Carbon dioxide	4.5 (99.995 vol %)
Ethane	3.5 (99.95 vol %)
Propane	3.5 (99.95 vol %)
Butane	2.5 (99.5 vol%)
Carbon monoxide	98 vol%
Hydrogen	5.0 (99.999 vol %)

Fig. 1. Flow scheme of the experimental setup used in this work.

2.2. Experimental Set-up

The lab-scale apparatus for determination of the reaction kinetics consists of a gas-mixing unit, a reactor with an electrical furnace and gas analyzer unit (see Fig. 1). The gases are supplied from standard gas cylinders. Gas composition is regulated by mass flow controllers. Water vapor can be added with a CEM-System (controlled evaporator mixer), both supplied by Bronkhorst High-Tech B.V. from Ruurlo, NL. The fixed bed reactor (1.4541 stainless steel) is divided into a preheating and a reaction zone with an inner diameter of 24 mm. The height of the catalyst bed varies between $h = 45$ mm and $h = 65$ mm. To avoid temperature gradients, the catalyst is diluted by Al_2O_3-spheres of equivalent diameter in a ratio of 1:10. The reaction temperature is measured with a multi- point thermocouple (K type; accuracy: $\pm 1.5\,°C$), located in the center of the catalyst bed. In order to prevent condensation in the subsequent gas analysis, a cooling trap is installed. Finally, the product gas composition is analyzed by a micro-GC (Agilent F490; MSA5 column; TCD; accuracy: $\pm 1\%$ F. S.) and an electrochemical oxygen transmitter (Pro-Chem-Analytik GmbH; range: 1–1,000 ppmv; accuracy: $\pm 2\%$ F.S.).

2.3. Experimental procedure

During the experiments, the gas inlet flow rate was varied in a range between 100 and 200 h^{-1} (STP), resulting in a GHSV (gas hourly space velocity) of 45,000 h^{-1} and 90,000 h^{-1}, respectively. The experiments were performed within a temperature range of $25 < T_R < 500\,°C$, a pressure range of $1 < p_{total} < 10$ bar and between 1,000 and 8,000 ppmv of oxygen in the feed gas stream. The kinetic measurements are evaluated at low oxygen feed concentrations, as a complete conversion of each 1,000 ppmv oxygen leads to an adiabatic temperature increase of about $10\,°C$. Therefore, it is unlikely that hot-spots in the catalyst bed are present at low oxygen feed concentrations. Thermal stability of the catalyst was checked regularly by monitoring the conversion of oxygen at a specific reproduction point. During the measurements, no catalyst deactivation effects were observed. Furthermore, carbon balance of oxidation reaction ($CH_4 \rightarrow CO_2$) has been monitored during the entire experimental program and indicates for the absence of any pyrolysis reactions in the examined temperature region. Besides, formation of CO by reforming reactions was not observed at any of the applied reaction conditions with the applied noble metal catalysts. The gas concentration at the reactor outlet was measured under stationary conditions. Steady state was assumed when the reaction temperature did not validate a temperature range of $\pm 0.5\,°C$ for at least 30 min. Experimental data points were generated by average determination of at least five separate GC measurements of the off gas composition.

3. Results and discussion

3.1. Control experiments

In preliminary experiments, the catalytic activity of the reaction system was examined to ensure that the experimental setup has no influence on the rate constants. The reactor was tested empty, with the sintered metal plate (catalyst bed support) included and finally with plate and the Al_2O_3-dilution material.

The results are shown in Fig. 2. The experiments without dilution material show no significant oxygen conversion. At $T_R = 500\,°C$ an overall oxygen conversion of 5% of the 1,000 ppmv of oxygen in the feed gas is observed, which is caused by the reactor itself. As the kinetic measurements have been performed in the temperature range below $350\,°C$, the reactor is presumed to be inert.

With the dilution material included, a complete conversion of oxygen occurs at $T_R = 500\,°C$. ICP-EOS measurements on the dilution material identified traces of ferrous compounds (<0.01 wt%), which are very likely to be responsible for the conversion of oxygen.
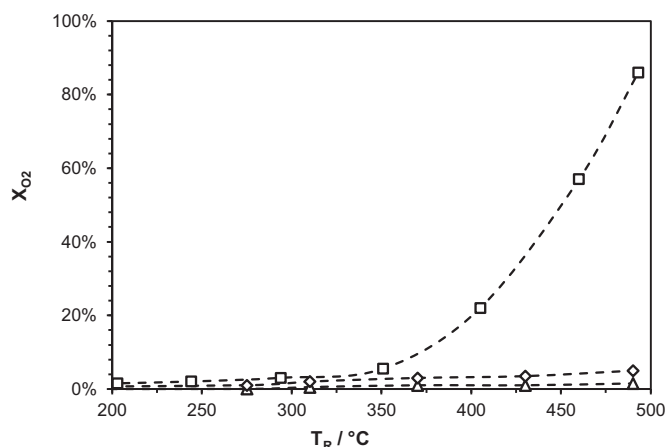
Fig. 2. Preliminary experiments on the catalytic activity of the experimental set-up ($\dot{V} = 100\,h^{-1}$ (STP), $p_{O_2,0} = 1$ mbar, GHSV: 45,000 h^{-1}, $p_{total} = 1.013$ bar, balance: CH_4): empty reactor ($\triangle$); empty reactor + metal plate ($\diamond$); empty reactor + plate + dilution material ($\square$).

Since $T_R = 350\,°C$ is the maximum reaction temperature of the kinetic measurements with the noble metal catalysts and less than 5% conversion of oxygen occurs at this temperature, the influence of the dilution material was neglected.

3.2. Removal of CH_4 from air vs. removal of O_2 from methane

In Fig. 3 operating conditions of a potential catalytic gas purification unit for removal of 2,000 ppmv and 4,000 ppmv of oxygen from methane rich gas streams (I) vs. temperature range for a catalytic exhaust gas treatment system for removal of 2,000 ppmv methane from air (II) are compared, using the same catalyst (Pt) and equivalent catalyst volumetric loading.

While the temperature for partial conversion ($X_i < 40\%$) does not differ significantly between both cases, for complete removal of oxygen in excess of methane considerably less temperature is necessary than for complete removal of methane from air streams. The conversion curve of methane removal from air (II) indicates, that the reaction rate decreases dramatically at high degrees of methane conversion (=low methane partial pressure). Therefore, for near 100% of methane conversion, about a 150 °C higher temperature has to be applied.
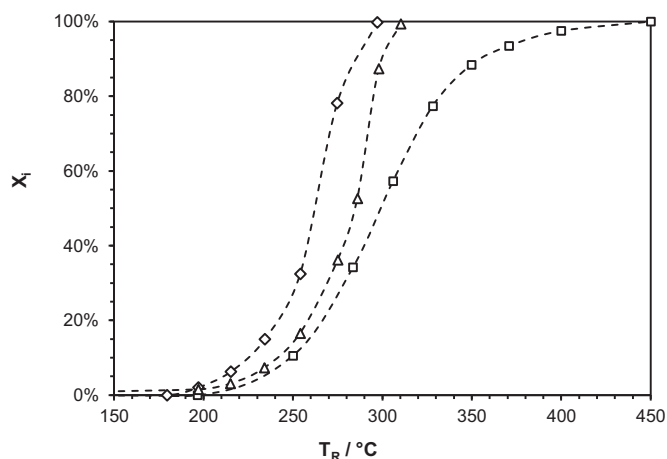
Fig. 3. Conversion of 2,000 ppmv methane in air ($\square$) vs. 2,000 ppmv O_2 ($\diamond$) and 4,000 ppmv O_2 ($\triangle$) in methane ($\dot{V} = 100\,h^{-1}$ (STP), GHSV: 45,000 h^{-1}, $p_{total} = 1.013$ bar).
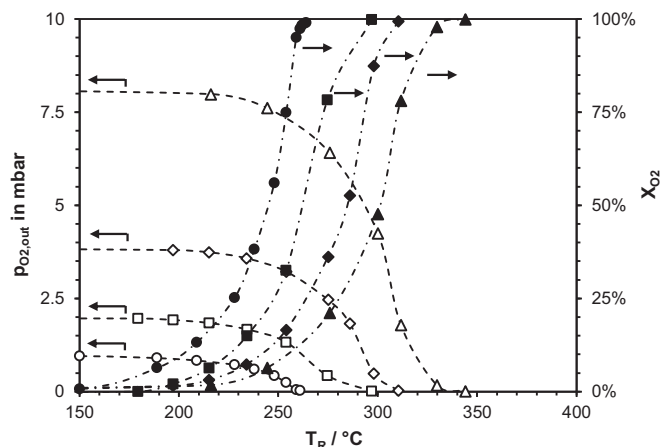
Fig. 4. Influence of oxygen partial pressure on the oxygen conversion ($\dot{V} = 100\,h^{-1}$ (STP), $pCH_4 = 960$ mbar, GHSV: 45,000 h^{-1}, $p_{total} = 1.013$ bar): $p_{O_2,0} = 1$ mbar ($\bullet$); 2 mbar ($\blacksquare$); 4 mbar ($\blacklozenge$); 8 mbar ($\blacktriangle$).

In this work, methane rich gas streams (Fig. 3: $\diamond$; $\triangle$) are of special interest. Hence combustion kinetics at methane partial pressures of up to 10 bar and low oxygen contents are examined.

### 3.3. Combustion of oxygen at excess methane conditions

3.3.1. Influence of oxygen partial pressure

In a first series of experiments, the influence of oxygen partial pressure on the total conversion of oxygen was investigated with platinum (Pt) as active compound. The experiments were performed in a range of oxygen inlet concentrations of 1,000–8,000 ppmv, corresponding to partial pressures of 1–8 mbar (when the reaction is carried out at atmospheric pressure). The partial pressure of methane at the inlet of the reactor was kept constant at 960 mbar during these experiments. The variation of oxygen content was compensated by adding nitrogen to an overall pressure of 1.013 bar. The results of these measurements are shown in Fig. 4.

For evaluation of the influence of p_{O_2} on the overall oxygen conversion, a comparison of total converted oxygen $n_{O_2,conv.}$ for a set of reaction temperatures gives an adequate visualization (see Fig. 5). While an increase of reaction temperature leads to a higher degree of oxygen conversion, partial pressure of O_2 has nearly no influence, as isotherms do not show a clear dependency of $p_{O_2,0}$ on $n_{O_2,conv.}$.
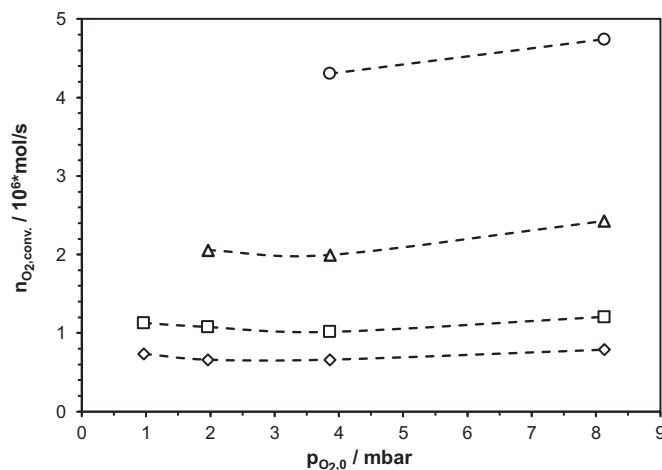
Fig. 5. Influence of $p_{O_2,0}$ (at the reactor inlet) on oxygen consumption for four different temperatures ($\dot{V} = 100\,h^{-1}$ (STP), $p_{CH_4,0} = 960$ mbar, GHSV: 45,000 h^{-1}, $p_{total} = 1.013$ bar): $T_R = 250\,°C$ ($\diamond$), 260 °C ($\square$), 270 °C ($\triangle$), 280 °C ($\bigcirc$).
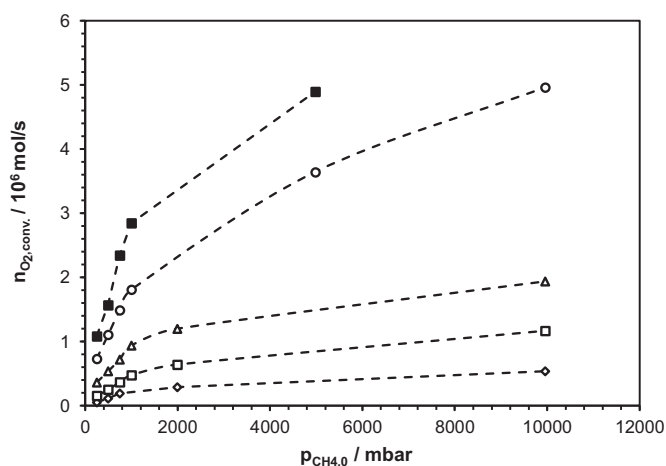
Fig. 6. Influence of $p_{CH_4,0}$ (at the inlet of the reactor) for five different temperatures ($\dot{V} = 100\,h^{-1}$ (STP), $y_{O_2,0} = 1{,}000$ ppmv, GHSV: $45{,}000\,h^{-1}$, $p_{total} = 1{-}10$ bar): $T_R = 218\,°C\,(\diamond)$, $237\,°C\,(\square)$, $256\,°C\,(\triangle)$, $278\,°C\,(\bigcirc)$, $289\,°C\,(\blacksquare)$

Fig. 7. Variation of $p_{O_2,0}$ and comparison with kinetic model ($\dot{V} = 100\,h^{-1}$ (STP), $p_{CH_4,0} = 960$ mbar, GHSV: $45{,}000\,h^{-1}$, $p_{total} = 1.013$ bar, balance: N_2): $p_{O_2,0} = 1$ mbar: exp ($\square$), calc (——); 2 mbar: exp ($\diamond$), calc (••••••••); 4 mbar: exp ($\triangle$), calc (– – – –); 8 mbar: exp($\bigcirc$), calc (— — -).

For stoichiometric and fuel lean mixtures equivalent observations are present in literature [12,26]. In such cases, Eley–Rideal is identified as an appropriate approach for modelling the catalytic oxidation of methane. The experimental results of this work illustrate that oxygen is still present in surplus on the catalytic surface, even at very low partial pressures. Indeed, the conversion curve for 1,000 ppmv oxygen (Fig. 4: ●) indicates that partial pressure of oxygen does not gain influence before $X_{O_2} \approx 95\%$ is reached, which corresponds to a partial pressure of $p_{O_2} = 5 \times 10^{-3}$ mbar.

### 3.3.2. Influence of methane partial pressure

Furthermore, oxygen conversion was studied at different partial pressures of methane. As methane is present in large surplus in the gas phase, conversion of methane is neglected and partial pressure of CH_4 is assumed to be constant in the reactor.

The isotherms in Fig. 6 show that the partial pressure of methane has a stronger influence on the conversion of oxygen than the partial pressure of oxygen.

Furthermore, the curves can be divided into two parts. At low methane partial pressures ($p_{CH_4,0} \leq 1$ bar), oxygen conversion shows a strong and linear increase with $p_{CH_4,0}$. Above $p_{CH_4,0} > 1$ bar, still an increase of conversion is observed. But the slope of the conversion curves reduces significantly at high methane partial pressures, indicating a change in predominant reaction step or in reaction mechanism.

In literature [27–30], the adsorption of methane (step I) or rather the following dissociation step in surface species (Pt–CH_3 and Pt–H, step II) are predominantly assumed to limit overall conversion rate. Saturation of the catalytic surface with methane is usually observed at high partial pressures, typically exceeding 10 bar [21]. However, results of this work indicate that for low oxygen concentrations, the transition point between predominance of methane adsorption (step I) and reaction kinetics limitation (step II) ranges around 1 bar of methane. This may be a result of reduced oxygen coverage on the catalysts surface, as in the examined case, oxygen concentration in the gas phase is substantially lower. Below 1 bar of methane in the gas phase, a linear trend of oxygen consumption vs. partial pressure of methane is observed. For a linear trend, the reaction order typically ranges around 1, as often reported in literature for fuel-lean mixtures in excess oxygen conditions [12,31].

Furthermore, the formation of by-products (CO, H_2, etc.) was continuously monitored with an online micro-GC. During the experiments with noble metals, no other reaction products than carbon dioxide and water have been detected.
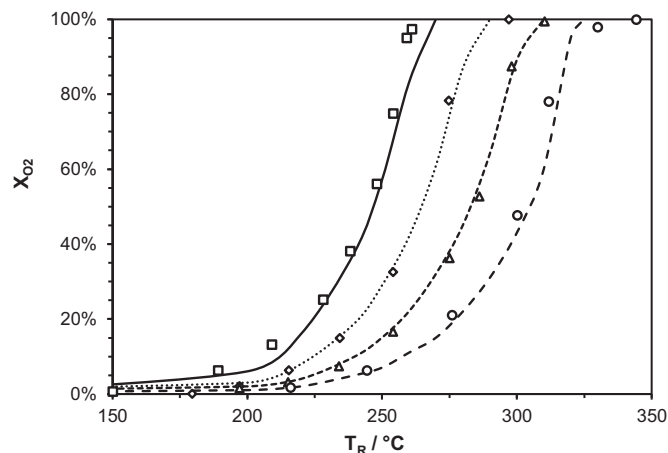
3.4. Reaction kinetics of oxygen conversion at excess methane conditions

For determination of the rate constants of the reaction, the experimental oxygen conversion data is analyzed. The reactor is assumed to be an isothermal, isobaric and ideal plug-flow reactor (Bo > 100). For the gas phase, a pseudo homogeneous model is assumed; only axial mass transport is taken into account. Mass transfer limitations in the catalyst pores are neglected (Wz < 1 for $T_R < 350\,°C$). The reaction rate (Eq. (4)) is based on the mass of active compound (ac). Inhibition terms are added to the rate equation in Section 3.5.

$$r_{m,O_2} = -\frac{1}{m_{ac}} \times \frac{dn_{O_2}}{dt} = k_0 \times \exp\left\{-\frac{E_A}{RT}\right\} \times 2\theta_{O_2} \times \theta_{CH_4} \qquad (4)$$

As methane is presumed to form only weak interactions with the catalyst surface at low partial pressures, a Freundlich adsorption isotherm is implemented, giving surface coverage of methane a dependency of CH_4 partial pressure in the power of B $\left(\theta_{CH_4} \sim p_{CH_4}^B\right)$.

Fig. 5 shows that oxygen partial pressure has nearly no influence on the reaction rate. As high oxygen surface coverage is assumed, a Langmuir adsorption isotherm is implemented and simplified to $\theta_{O_2} \sim p_{O_2}^A$ with $A = 0$ for $p_{O_2} \ll 1$ bar. While kinetic parameters were evaluated, the reaction order in oxygen (A) was still kept as an additional degree of freedom, indicating, whether the assumption of high oxygen surplus on the catalysts surface and therefore the applicability of common models (e.g., Eley–Rideal) is valid for the biogas case.

The kinetic parameters and reaction orders in oxygen and methane were determined by numeric fit via minimization of least squares of integral experimental and calculated oxygen conversion. The gradient of oxygen concentration along the catalyst bed was taken into account, as a reactor model (a series of N > 100 CSTR) was implemented and oxygen conversion was calculated along the catalyst layer. MS Excel was used for computation. As reaction orders and kinetic constants interact, the data sets on variation of oxygen and methane pressures were used for evaluation of kinetic parameters.

Experimental data and the results of kinetic modelling show good agreement (see Figs. 7 and 8). The reaction order in methane B for $p_{CH_4,0} \leq 1$ bar was calculated to 0.95. The reaction order in oxygen A was 0.04 (and therefore set to 0). Consequently, this observation indicates that the adsorption of methane is the rate determining step of the reaction process in this pressure range,

Table 4
Kinetic data for methane as a reducer for oxygen for two pressure ranges.

Reducer	p_{CH4}	A	B	$k_{0,thiswork}$	$E_{A,thiswork}$
Methane	$p_{CH_4} \leq 1$ bar	0	0.95	$(1.2 \pm 0.7) \cdot 10^8$ mol/(kg s bar^B)	90.3 ± 4 (kJ/mol)
Methane	1 bar < $p_{CH_4} \leq 10$ bar	0	0.38		
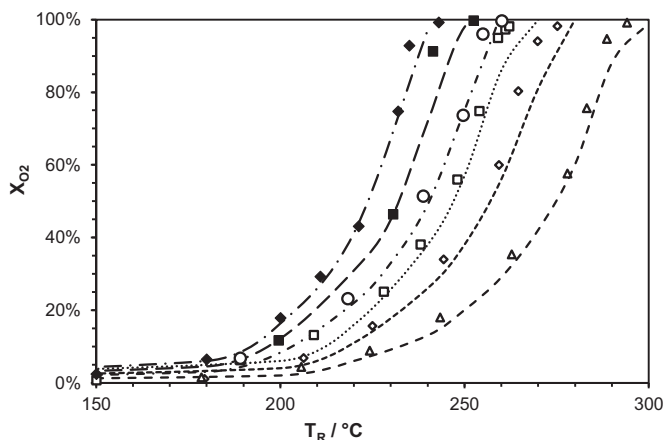
Fig. 8. Variation of p_{CH_4} and comparison with kinetic model ($\dot{V} = 100\,h^{-1}$ (STP), $y_{O_2,0} = 1000$ ppmv, GHSV: $45,000\,h^{-1}$, $p_{total} = 1–10$ bar, balance: N$_2$): $p_{CH_4} = 960$ mbar: exp (□), calc (········); 660 mbar: exp (◊), calc (━ ━ ━); 330 mbar: exp (△), calc (━ ━ ━); 1,990 mbar: exp (○), calc (━ · ━ ·); 4,975 mbar: exp (■), calc (━━ ━━); 9,950 mbar: exp (◆), calc (━━ · ·).

Fig. 9. Inhibiting effect of CO$_2$ on oxygen conversion ($\dot{V} = 100\,h^{-1}$ (STP), $p_{O_2,0} = 2$ mbar, GHSV: $45,000\,h^{-1}$, $p_{total} = 1.013$ bar): $p_{CH_4} = 745$ mbar in N$_2$ (□); $p_{CH_4} = 745$ mbar in CO$_2$ (■); $p_{CH_4} = 245$ mbar in N$_2$ (△); $p_{CH_4} = 245$ mbar in CO$_2$ (▲).

which allows for an expansion of validity range of Eley–Rideal mechanism down to very low partial pressures of oxygen. For methane pressures $p_{CH_4,0}$ of 1–10 bar, the reaction order was calculated to 0.38. In this range, methane still has limiting influence on the reaction rate, but surface coverage of methane shows beginning of a saturation trend, which becomes predominant at $p_{CH_4,0} > 10$ bar [21]. The determined kinetic parameters of interest are given in Table 4.

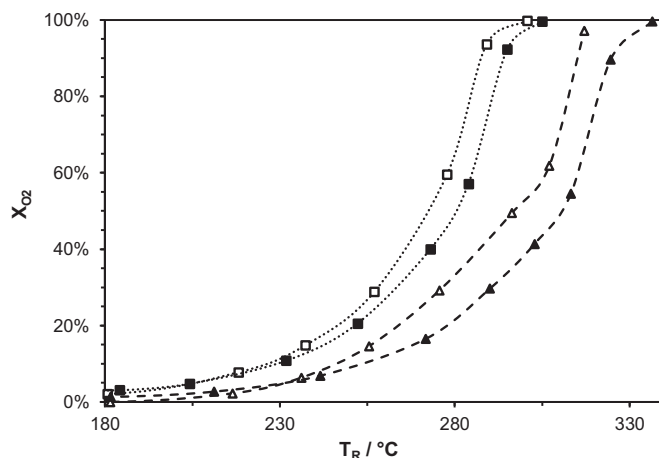The activation energy for the reaction was calculated to 90.3 kJ/mol for both pressure ranges. The result is similar to many citations ($E_A \approx 70–110$ kJ/mol [12,32–34]), indicating that the same reaction mechanism can be applied for excess methane conditions.

3.5. Inhibition effects on reaction kinetics

3.5.1. Influence of carbon dioxide

Carbon dioxide is one of the two major reaction products of the total oxidation of methane. In the present case, where the reaction is used as a purification step for low oxygen contents, only small amounts of carbon dioxide are formed. But, depending on the positioning of a potential oxygen removal unit in the biogas treatment process, carbon dioxide contents of up to 50 vol% can occur in the inlet gas stream. To identify and quantify a potential inhibition effect of carbon dioxide experiments with different concentrations of carbon dioxide were carried out. Fig. 9 gives a direct comparison for different partial pressures of methane, as nitrogen and carbon dioxide were used as balance alternately. The oxygen content ($p_{O_2,0} = 2$ mbar) was kept constant during these experiments.

As shown in Fig. 9, carbon dioxide has a weak inhibiting effect on oxygen conversion, visible in the slightly higher temperatures needed for equivalent conversion of oxygen. The influence of carbon dioxide on the reaction kinetics is taken into account by an inhibition term with a reaction order in partial pressure of CO$_2$ of −2.5. To deal with units, a temperature invariant constant K_{CO_2} with

value of 1 bar$^{2.5}$ is added. As can be seen in Fig. 10, comparison between experimental and calculated data shows good agreement.

$$r_{m,O_2} = f\left(K_{CO_2} p_{CO_2}^{-2.5}\right) \tag{5}$$

The results are not clearly comparable with other authors data. While an inhibiting effect of CO$_2$ is often, but not always [25], observed, the determined reaction order varies strongly. The partial pressures of the reactants have a crucial impact [35–37]. The inhibiting effect of carbon dioxide becomes more visible, when partial pressure of methane is comparably low. Therefore, it can be stated that the adsorption of carbon dioxide competes with methane adsorption and consequently reduces the reaction rate of methane combustion.
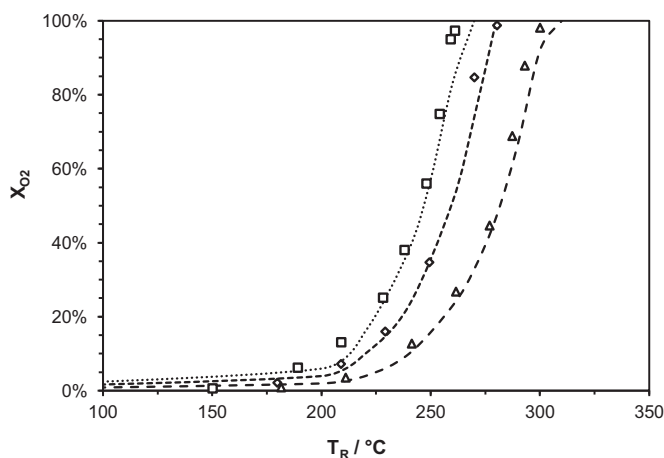
Fig. 10. Variation of p_{CO_2} and comparison with kinetic model ($\dot{V} = 100\,h^{-1}$ (STP), $p_{O_2,0} = 1$ mbar, GHSV: $45,000\,h^{-1}$, balance: CH$_4$; $p_{total} = 1.013$ bar): $p_{CO_2} = 0$ mbar: exp (□), calc (········); 330 mbar: exp (◊), calc (━ ━ ━); 660 mbar: exp (△), calc (━ ━ ━).
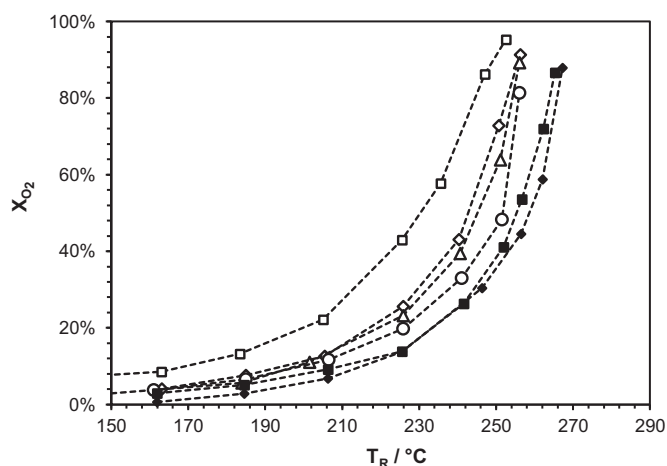
Fig. 11. Inhibiting effect of water vapor on oxygen conversion ($\dot{V}$ = 100 h^{-1} (STP), $p_{O_2,0}$ = 1 mbar, GHSV: 45,000 h^{-1}, p_{CH_4} = 960 mbar, p_{total} = 1.013 bar): p_{H_2O} = 0 mbar (□); 2 mbar (◇); 5 mbar (△); 10 mbar (○); 20 mbar (■); 30 mbar (♦); balance: N$_2$.

Fig. 12. Variation of p_{H_2O} and comparison with kinetic model ($\dot{V}$ = 100 h^{-1} (STP), $p_{O_2,0}$ = 1 mbar, GHSV: 45,000 h^{-1}, p_{CH_4} = 960 mbar, p_{total} = 1.013 bar): p_{H_2O} = 2 mbar: exp (■), calc (⋯⋯); 2 mbar: exp (♦), calc (━ ━ ━); balance: N$_2$.

3.5.2. Influence of water vapor

The second major reaction product is water. Therefore, the influence of water vapor in the feed gas on the oxygen conversion has been studied. Corresponding to typical biogas compositions, the partial pressure of water vapor was varied in a range of p_{H_2O} = 2–30 mbar. Methane (p_{CH_4} = 960 mbar) and oxygen ($p_{O_2,0}$ = 1 mbar) contents were kept constant. The results are shown in Fig. 11.

Adding water vapor to the feed gas requires an increase in reaction temperatures for equal oxygen conversion in comparison to dry gas. The presence of water vapor inhibits the reaction stronger than carbon dioxide does. Furthermore, it is remarkable, that even at very low partial pressures of H$_2$O, the decrease of oxygen conversion is stronger than the inhibiting effect of carbon dioxide at high contents.

This effect is also observed in the literature [25] and often explained by a multilayer adsorption of water on the catalyst surface [38]. The inhibiting effect gains significance with a decrease in temperature, a high total pressure and an increasing partial pressure of water vapor. The reaction order is often presumed in a range of −0.75 to −1 [21,38].

In this work, the inhibition effect, caused by water vapor is taken into account by a temperature-dependent adsorption constant $K_{H_2O}(T)$. The implementation of a BET-adsorption isotherm, as often used in literature, does not result in a better fit of experimental data for the examined range of water contents. The temperature dependence of the adsorption constant is described by Eq. (6).

$$K_{H_2O}(T) = K_{H_2O,0} \times \exp\left(\frac{-\Delta_{ads}H^0}{RT}\right) \qquad (6)$$

The fit leads to a reaction order in water vapor of −0.5 and a heat of adsorption for water on the catalyst surface of 59 kJ/mol, which is in good agreement with the heat of adsorption of water on an alumina surface [39] (Eq. (7)).

$$r_{m,O_2} = f\left(\frac{1}{K_{H_2O}(T) \times p_{H_2O}^{0.5}}\right) \qquad (7)$$

Fig. 12 shows a comparison of experimental and calculated data for 2 mbar and 20 mbar of water vapor in the feed gas at the inlet of the catalytic reactor.
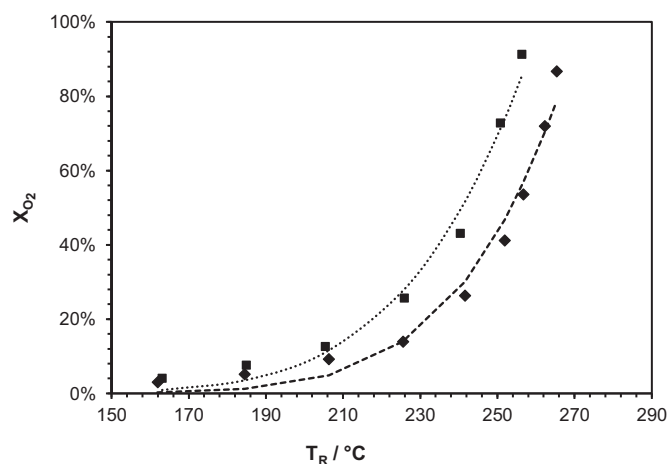
### 3.6. Variation of catalyst load and residence time

For determination of catalyst load and gas residence times influence on the overall conversion of oxygen, several experiments were carried out. To evaluate both effects separately, total gas flow rate and mass flow of oxygen in the inlet stream were varied independently. In order to increase the catalyst load (GHSV), the volumetric flow rate was doubled, while catalyst mass was kept constant (see Fig. 13).

As expected, an increase in flow rate of the feed gas necessitates higher temperatures for equal oxygen conversion. Constant mole flow of oxygen, however, results in equal reaction temperatures, even if the gas flow rate is doubled. This observation indicates that the fixed-bed configuration used in this work is isothermal in good approximation and the heat of combustion can be removed from the reaction system effectively.

Furthermore, the results confirm the aforementioned observation of a strong oxygen affinity to the catalysts active compound, which is very likely the reason for the insignificant influence of hydraulic gas residence times on oxygen conversion in the studied case.
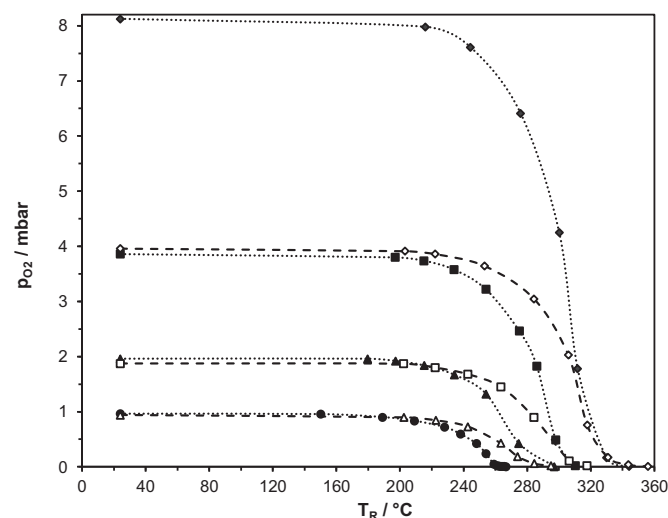
Fig. 13. Influence of catalyst load on oxygen conversion (p_{CH_4} = 960 mbar, p_{total} = 1.013 bar): GHSV: 45,000 h^{-1}: $p_{O_2,0}$ = 8 mbar (♦), 4 mbar (■), 2 mbar (▲), 1 mbar (●); GHSV: 90,000 h^{-1}: $p_{O_2,0}$ = 4 mbar (◇), 2 mbar (□), 1 mbar (△); balance: N$_2$.
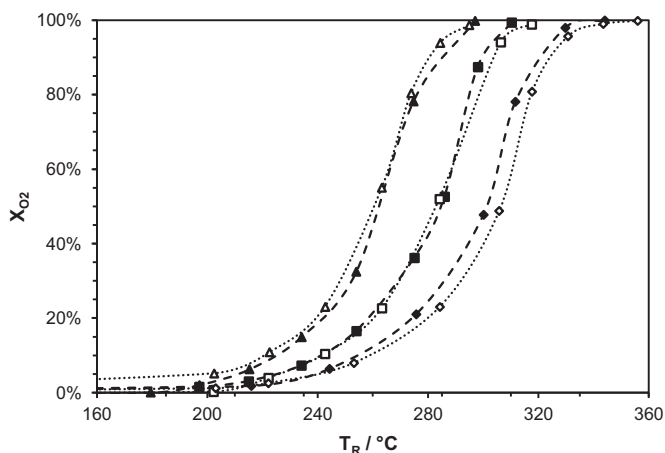
Fig. 14. Influence of catalyst load on oxygen conversion (p_{CH_4} = 960 mbar, p_{total} = 1.013 bar): GHSV: 45,000 h^{-1}: $p_{O_2,0}$ = 8 mbar (♦), 4 mbar (■), 2 mbar (▲); GHSV: 90,000 h^{-1}: $p_{O_2,0}$ = 4 mbar (◊), 2 mbar (□), 1 mbar (△); balance: N$_2$.

Fig. 14 points out this effect, as oxygen conversion curves for equal total moles of oxygen in the feed gas correspond, even though feed gas flow is doubled.

### 3.7. Combustion kinetics for alternative reducing agents

Besides methane, other reductants, e.g., further hydrocarbons, carbon monoxide or hydrogen can be used for catalytic removal of oxygen from (bio-) gas streams. Fig. 15 illustrates the conversion of various alternative fuels in comparison to methane.

In accordance with literature [32,40], higher hydrocarbons require a lower reaction temperature than methane. The increase in reactivity is caused by the higher proportion of secondary C—H bonds in the fuel molecules, which can be cracked at lower temperatures.

For modelling the reaction rate of alternative fuels, a power law approach was used (Eq. (8)).

$$r_{O_2,i} = k_{0,i} \times \exp\left(\frac{-E_{A,i}}{RT}\right) \times p_{O_2}^{A_i} \times p_i^{B_i} \tag{8}$$

The reaction order in oxygen was set to zero, the reaction order in the fuel components and the kinetic constants were determined by variation of gas composition, similar to the approach with methane, inhibition terms were not applied.
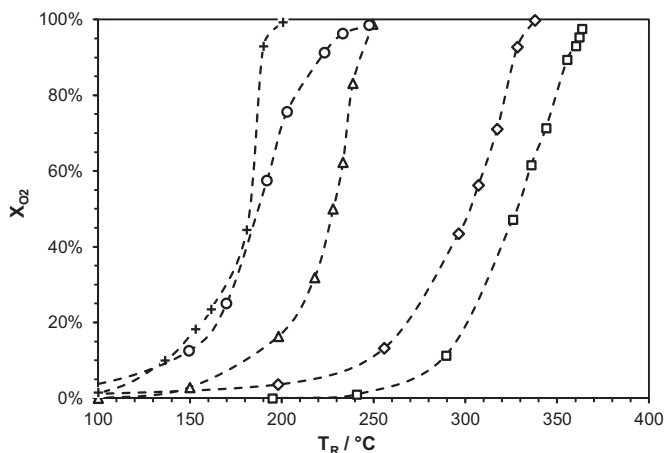
Fig. 15. Oxygen conversion of various reductants ($\dot{V}$ = 100 h^{-1} (STP), $p_{O_2,0}$ = 1 mbar; p_{red} = 2 mbar, GHSV: 45,000 h^{-1}, p_{total} = 1.013 bar, balance: N$_2$): methane (□); ethane (◊); propane (△); CO (○); butane (+).
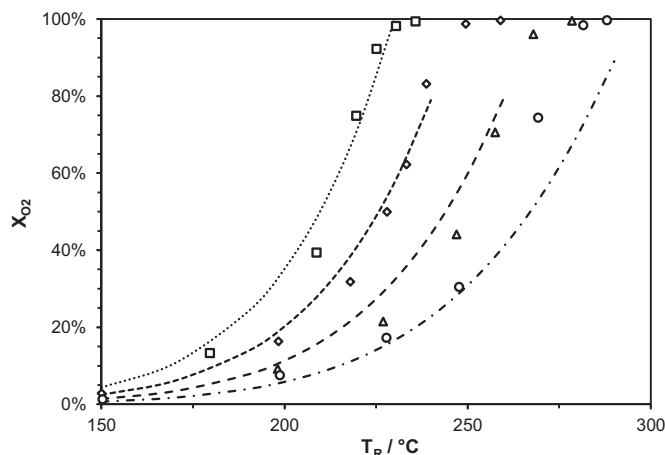
Fig. 16. Variation of $p_{propane}$ and comparison with kinetic model ($\dot{V}$ = 100 h^{-1} (STP), GHSV: 45,000 h^{-1}, p_{total} = 1.013 bar): $p_{propane}$ = 5 mbar, $p_{O_2,0}$ = 1 mbar: exp (□), calc (⋯⋯); $p_{propane}$ = 2.5 mbar, $p_{O_2,0}$ = 1 mbar: exp (◊), calc (— — —); $p_{propane}$ = 1.25 mbar, $p_{O_2,0}$ = 1 mbar: exp (△), calc (— — •); $p_{propane}$ = 1.25 mbar, $p_{O_2,0}$ = 2 mbar: exp (○), calc (— • —); balance: N$_2$.

Table 5
Kinetic data for various alternative reducing agents.

Reductant	A	B	$E_{A,thiswork}$ (kJ/mol)	$E_{A,Lit}$ [41] (kJ/mol)	$E_{A,Lit}$ [40] (kJ/mol)
Ethane	0	0.47	95.3 ± 3	114.7	108.9
Propane	0	0.83	69.6 ± 2	97.9	92.1
Butane	0	0.82	72.7 ± 2	71.4	104.7

As shown in Fig. 16, experimental data and the modelling of oxygen conversion for e.g., propane are in good agreement.

Similar to methane, the reaction accelerates as partial pressure of the reductant is increased. The influence of oxygen partial pressure is stronger than for methane due to an increasing oxygen demand at the active sites of the catalyst surface. Still, reaction order of oxygen was set to zero, as this presumption is often found in the literature [21]. The determined rate constants for alternative fuels are shown in Table 5.

The conversion of carbon monoxide to carbon dioxide occurs at reaction temperatures in between of propane and butane. Complete removal of oxygen ($p_{O_2,0}$ = 1 mbar) with hydrogen ($p_{H_2,0}$ = 2.5 mbar) was possible near ambient temperature, only 40–50 °C were necessary. Due to the small temperature difference between the catalytic reactor and ambient laboratory temperature, it is not possible to dissipate enough heat from the reactor. Thus, a temperature controlled conversion experiment with hydrogen was not realizable in the experimental set-up used, as there is no possibility to cool the reactor system actively.

3.8. Comparison of Pt with other catalyst materials

Additionally, alternative catalyst materials were studied in comparison to platinum, which was used as a reference for catalyst activity. In order to ensure comparability between the different materials, the GHSV was kept constant.

While noble metals like platinum or palladium feature a high catalytic activity, other transition metals like copper require higher reaction temperatures for complete conversion of oxygen (see Fig. 17). While rhodium features a higher activity, the application of copper based catalyst exhibits economic benefits. The silver catalyst does not perform better than the dilution material, indicating that thermal decomposition occurs with this catalyst. The focus of catalyst optimization for this application has to be identifying an
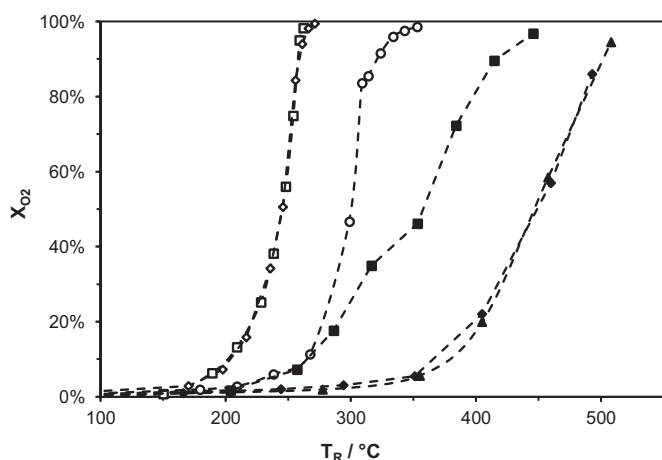
Fig. 17. Oxygen conversion on various catalysts ($\dot{V} = 100\,h^{-1}$ (STP), $p_{CH_4} = 960$ mbar, $p_{O_2,0} = 1$ mbar, GHSV: 45,000 h^{-1}, $p_{total} = 1.013$ bar, balance: air): Pt (□); Pd (◇); Rh (○); Cu (■); Ag (▲); Al$_2$O$_3$ (♦).

optimum between costs, performance and durability in respect to the critical minor constituents of biogas.

4. Summary and conclusion

For basic engineering of catalytic units for the removal of oxygen from biogas streams by oxidation of methane, examinations on reaction kinetics have been carried out in a lab scale experimental setup.

In comparison with other reductants, e.g., hydrogen, carbon monoxide or hydrocarbons (C_nH_{2n+2} with $2 \leq n \leq 4$), methane features the highest stability of all tested reducing agents and therefore requires the highest reaction temperature to reduce oxygen.

In case methane-rich gas streams are used (e.g., when natural gas or biogas are to be purified), the required reaction temperature is lower than for the removal of methane from exhaust gas streams. The reaction can be performed in a temperature range below 350 °C for typical oxygen inlet concentrations. On the basis of the experimental results, a mass based rate equation is proposed, taking into account the influence of both, reactants and products of the reaction (see Eq. (9)), on the conversion rate of oxygen.

$$r_{m,O_2} = k_{O_2}(T) \times p_{CH_4}^B \times \frac{1}{\left(1 + K_{CO_2} p_{CO_2}^{2.5} + K_{H_2O}(T) \times p_{H_2O}^{0.5}\right)} \quad (9)$$

This equation is valid for oxygen inlet pressures $p_{O_2,0}$ in the range of 1–10 mbar and has further been tested in a balance of methane of up to 10 bar (abs.). For the partial pressure range of methane $p_{CH_4} \leq 1$ bar the reaction order in methane was calculated to 0.95. For $1 < p_{CH_4} < 10$ bar the reaction order in methane is 0.38. With these parameters, calculated oxygen conversion is in good agreement with the experimental data within the examined range of operating conditions.

The reaction further shows no significant dependence on gas hydraulic residence time. This is due to the fact, that the applied noble metal catalyst shows a strong affinity for oxygen. Methane, however, is present in high content in any of the examined cases.

For estimation of conversion rates of ethane, propane and butane in comparison to the conversion of oxygen with methane, power law approaches were applied and kinetic parameters are given.

Finally, the catalytic activity of some alternative noble metal catalysts and some transition metal catalysts was tested and compared to the platinum reference catalyst. As expected, noble metal catalysts feature the highest activity, but are also the most expensive

materials. Hence, the selection of an appropriate catalyst material is an economic problem, for which CAPEX of the oxygen removal unit and other factors, e.g. catalyst durability etc., have to be taken into consideration.

References

[1] FNR. e.V., Biogasanlagen zur Biomethanproduktion in Deutschland, available at <http://mediathek.fnr.de>, 2014.
[2] T. Muschalle, M. Amro, DGMK Research Report 753: Influence of Oxygen Impurities on Underground Gas Storage and Surface Equipment, 2013.
[3] DVGW e. V., G 260 Gasbeschaffenheit, 2013.
[4] DVGW e.V., G 262 Nutzung von Gasen aus regenerativen Quellen in der öffentlichen Gasversorgung, 2011.
[5] EASEE-Gas, CBP 2005-001/02: Harmonisation of Natural Gas Quality, 2005.
[6] W. Köppel, F. Graf, Results of a DVGW biogas monitoring program, gwf-Gas|Erdgas Int. 151 (13) (2010) 38–46.
[7] W. Köppel, et al., Vermeidung und Entfernung von Sauerstoff bei der Einspeisung von Biogas in das Erdgasnetz, gwf-Gas|Erdgas 153 (1) (2012) 2–11.
[8] A.L. Kohl, R.B. Nielsen, Gas Purification, 5th ed., Gulf Pub., Houston, 1997.
[9] B.H. Engler, Katalysatoren für den Umweltschutz, CIT 63 (1991) 298–312.
[10] J.N. Armor, Energy efficiency and the environment opportunities for catalysis, Appl. Catal. A: Gen. 194–195 (2000) 3–11.
[11] T.R. Baldwin, R. Burch, Catalytic combustion of methane over supported palladium catalysts, Appl. Catal. 66 (1990) 337–358.
[12] P. Hurtado, S. Ordóñez, A. Vega, F.V. Díez, Catalytic combustion of methane over commercial catalysts in presence of ammonia and hydrogen sulphide, Chemosphere 55 (5) (2004) 681–689.
[13] P. Gélin, M. Primet, Complete oxidation of methane at low temperature over noble metal based catalysts: a review, Appl. Catal. B: Environ. 39 (1) (2002) 1–37.
[14] V.R. Choudhary, B.S. Uphade, S.G. Pataskar, A. Keshavaraja, Low-temperature complete combustion of methane over Mn-, Co-, and Fe-stabilized ZrO$_2$, Angew. Chem. Int. Ed. Engl. 35 (20) (1996) 2393–2395.
[15] E. Garbowski, M. Guenin, M.-C. Marion, M. Primet, Catalytic properties and surface states of cobalt-containing oxidation catalysts, Appl. Catal. 64 (1990) 209–224.
[16] D. Döbber, D. Kießling, W. Schmitz, G. Wendt, MnO$_x$/ZrO$_2$ catalysts for the total oxidation of methane and chloromethane, Appl. Catal. B: Environ. 52 (2) (2004) 135–143.
[17] S. Tanaka, K. Nakagawa, E. Kanezaki, M. Katoh, K.-I. Murai, T. Morigai, I. Nakabayashi, S. Sugiyama, Y. Kidoguchi, K. Miwa, Catalytic activity of iron oxides supported on γ- Al$_2$O$_3$ for methane oxidation, J. Jpn. Pet. Inst. 48 (4) (2005) 223–228.
[18] L. Marchetti, L. Forni, Catalytic combustion of methane over perovskites, Appl. Catal. B: Environ. 15 (3–4) (1998) 179–187.
[19] M. Schmal, Mariana M.V.M. Souza, V.V. Alegre, Mônica Antunes Pereira da Silva, D.V. César, Carlos A.C. Perez, Methane oxidation–effect of support, precursor and pretreatment conditions–in situ reaction XPS and DRIFT, 5th International Symposium on Group 5 Compounds 118 (3–4) (2006) 392–401.
[20] J. Koop, O. Deutschmann, Detailed surface reaction mechanism for Pt-catalyzed abatement of automotive exhaust gases, Appl. Catal. B: Environ. 91 (1–2) (2009) 47–58.
[21] F.W. Knebel, Erdgasvorwärmung durch direkte katalytische Oxidation: Inline-Gasvorwärmung. Dissertation, Karlsruhe, 2000.
[22] P. Aghalayam, Y.K. Park, N. Fernandes, V. Papavassiliou, A.B. Mhadeshwar, D.G. Vlachos, A C1 mechanism for methane oxidation on platinum, J. Catal. 213 (1) (2003) 23–38.
[23] P. Hurtado, S. Ordóñez, H. Sastre, F.V. Díez, Development of a kinetic model for the oxidation of methane over Pd/Al$_2$O$_3$ at dry and wet conditions, Appl. Catal. B: Environ. 51 (4) (2004) 229–238.
[24] A.D. Mayernick, M.J. Janik, Methane oxidation on Pd-Ceria: a DFT study of the mechanism over Pd$_x$Ce$_{1-x}$O$_2$, Pd, and PdO, J. Catal. 278 (1) (2011) 16–25.
[25] J.C. van Giezen, F.R. van den Berg, J.L. Kleinen, A.J. van Dillen, J.W. Geus, The effect of water on the activity of supported palladium catalysts in the catalytic combustion of methane, Catal. Today 47 (1–4) (1999) 287–293.
[26] J.H. Lee, D.L. Trimm, Catalytic combustion of methane, Trends Nat. Gas Utilisation 42 (2–3) (1995) 339–359.
[27] A.C. Luntz, H.F. Winters, Dissociation of methane and ethane on Pt(110): evidence for a direct mechanism under thermal conditions, J. Chem. Phys. 101 (12) (1994) 10980–10989.
[28] D.A. Hickman, L.D. Schmidt, Steps in CH$_4$ oxidation on Pt and Rh surfaces: high- temperature reactor simulations, AIChE J. 39 (7) (1993) 1164–1177.
[29] G.R. Schoofs, C.R. Arumainayagam, M.C. McMaster, R.J. Madix, Dissociative chemisorption of methane on Pt(111), Surf. Sci. 215 (1–2) (1989) 1–28.

[30] K. Otto, Methane oxidation over Pt on.gamma.-alumina: kinetics and structure sensitivity, Langmuir 5 (6) (1989) 1364–1369.

[31] A. Janbey, W. Clark, E. Noordally, S. Grimes, S. Tahir, Noble metal catalysts for methane removal, Chemosphere 52 (6) (2003) 1041–1046.

[32] T.F. Garetto, C.R. Apesteguía, Oxidative catalytic removal of hydrocarbons over Pt/Al$_2$O$_3$ catalysts, Catal. Today 62 (2–3) (2000) 189–199.

[33] J.M. Jones, V.A. Dupont, R. Brydson, D.J. Fullerton, N.S. Nasri, A.B. Ross, A.V.K. Westwood, Sulphur poisoning and regeneration of precious metal catalysed methane combustion, Catal. Today 81 (4) (2003) 589–601.

[34] P.G. Tsyrulnikov, V.S. Sal'nikov, V.A. Drozdov, A.S. Noskov, N.A. Chumakova, V.K. Ermolaev, I.V. Malakhova, Deep oxidation of methane on alumina–manganese and Pt-containing catalysts, J. Catal. 198 (2) (2001) 164–171.

[35] U. Feuerriegel, W. Klose, S. Sloboshanin, H. Goebel, J.A. Schaefer, Deactivation of a palladium-supported alumina catalyst by hydrogen sulfide during the oxidation of methane, Langmuir 10 (10) (1994) 3567–3570.

[36] R. Burch, F.J. Urbano, P.K. Loader, Methane combustion over palladium catalysts: the effect of carbon dioxide and water on activity, Appl. Catal. A: Gen. 123 (1) (1995) 173–184.

[37] O.P. Ahuja, G.P. Mathur, Kinetics of catalytic oxidation of methane: application of initial rate technique for mechanism determination, Can. J. Chem. Eng. 45 (6) (1967) 367–371.

[38] M. Reinke, Katalytisch stabilisierte Verbrennung von CH$_4$/Luft Gemischen und H$_2$O- und CO$_2$-verdünnten CH$_4$/Luft Gemischen über Platin unter Hochdruckbedingungen. Dissertation, Zürich, 1971.

[39] P.W. Atkins, J. de Paula, Kurzlehrbuch Physikalische Chemie: Elements of Physical Chemistry, 4th ed., Wiley- VCH, Weinheim, 2008.

[40] Y.-F.Y. Yao, Oxidation of alkanes over noble metal catalysts, Ind. Eng. Chem. Prod. Res. Dev. 19 (3) (1980) 293–298.

[41] M. Aryafar, F. Zaera, Kinetic study of the catalytic oxidation of alkanes over nickel, palladium, and platinum foils, Catal. Lett. 48 (3–4) (1997) 173–183.